SIMULATION OF PHYSICAL PROCESSES

Original article
DOI: https://doi.org/10.18721/JPM.16405

A COMPARISON OF TWO APPROACHES TO THE GLOBAL STABILITY ANALYSIS USING THE EXAMPLE OF THE CYLINDER FLOW PROBLEM

V. D. Golubkov✉, *A. V. Garbaruk*

Peter the Great St. Petersburg Polytechnic University, St. Petersburg, Russia

✉ golubkovvd@gmail.com

Abstract. In the paper, the two main approaches to calculating the Jacobian of the Navier–Stokes equations, namely, the continuum (CA) and discrete (DA) approaches, have been directly compared for the first time. The DA to calculating this Jacobian was implemented based on in-house finite-volume code for hydrodynamics simulation (in addition to the already existing CA). The DA was successfully verified by comparison between the obtained numerical result and that of solving the transient Navier–Stokes equations. The comparison of these approaches was carried out using the example of a laminar flow past a cylinder by a perfect gas at the near-critical Reynolds numbers (Re = 50 and 60). It was established that the CA predicted the growth rate of perturbations more accurately, while the DA did their frequency and amplitude in toto. The results obtained allow to assert that both CA and DA are equivalent in terms of accuracy, and the choice of a particular approach for analyzing the stability may determine by other criteria, e. g., ease of implementation, computational work and so on.

Keywords: global stability analysis, Navier–Stokes equations, Jacobian, automatic differentiation

Funding: The reported study was funded by Russian Science Foundation (Grant No. 22-11-00041).

Citation: Golubkov V. D., Garbaruk A. V., A comparison of two approaches to the global stability analysis using the example of the cylinder flow problem, St. Petersburg State Polytechnical University Journal. Physics and Mathematics. 16 (4) (2023) 50–62. DOI: https://doi.org/10.18721/JPM.16405

Научная статья
УДК 532.5.013.4
DOI: https://doi.org/10.18721/JPM.16405

СРАВНЕНИЕ ДВУХ ПОДХОДОВ К ГЛОБАЛЬНОМУ АНАЛИЗУ ГИДРОДИНАМИЧЕСКОЙ УСТОЙЧИВОСТИ НА ПРИМЕРЕ ЗАДАЧИ ОБТЕКАНИЯ ЦИЛИНДРА

В. Д. Голубков✉, *А. В. Гарбарук*

Санкт-Петербургский политехнический университет Петра Великого,

Санкт-Петербург, Россия

✉ golubkovvd@gmail.com

Аннотация. В работе впервые проведено прямое сравнение двух основных подходов к вычислению якобиана уравнений Навье – Стокса: континуального (КП) и дискретного (ДП). На базе собственного конечно-объемного кода для моделирования течений реализован ДП к вычислению якобиана (в дополнение к уже существующему КП). ДП был успешно верифицирован путем сравнения полученного численного результата с решением нестационарных уравнений Навье – Стокса. Сравнение двух подходов проведено на примере ламинарного обтекания цилиндра идеальным газом при околокритических числах Рейнольдса (Re = 50 и 60). Установлено, что КП точнее предсказывает показатель роста возмущений, а ДП – их частоту и амплитуду в целом. Полученные результаты позволяют утверждать, что КП и ДП равнозначны по порядку точности и выбор конкретного подхода для проведения анализа устойчивости может определяться другими критериями (например, простота реализации, вычислительные затраты и др.).

Ключевые слова: глобальный анализ устойчивости, якобиан уравнений Навье – Стокса, автоматическое дифференцирование

Финансирование: Работа выполнена при финансовой поддержке Российского научного фонда (грант № 00041-11-22).

Ссылка для цитирования: Голубков В. Д., Гарбарук А. В. Сравнение двух подходов к глобальному анализу гидродинамической устойчивости на примере задачи обтекания цилиндра // Научно-технические ведомости СПбГПУ. Физико-математические науки. 2023. Т. 16. № 4. С. 50–62. DOI: https://doi.org/10.18721/JPM.16405

Introduction

One of the most powerful and advanced tools for studying the stability of viscous fluid flows is the linear theory of stability, which considers the development of small perturbations that do not interact with each other. Most 20th century studies were based on the linear theory of hydrodynamic stability within the framework of the locally parallel approach (the Orr–Sommerfeld equation) or two-dimensional parabolized equations (see books [1, 2] and a review [3]). By the end of the 20th century, the advances in computer technologies made it possible to conduct linear stability analysis of two-dimensional and even three-dimensional solutions of the Navier–Stokes equations; this approach came to be known as global stability analysis (GSA) in the literature [4].

The dynamics of the evolution of small perturbations within the GSA is determined by the matrix of derivatives of the governing equations with respect to all variables, i.e. the Jacobian of the stationary Navier–Stokes equations (more precisely, its discrete form). Currently, two different approaches are used to calculate this Jacobian. For example, [5–9] covering a wide range of problems of GSA for two-, three- and quasi-three-dimensional flows used the approach called continuum in [10]. It consists in the initial linearization of the Navier–Stokes equations, which leads to an analytical expression for their Jacobian, for which a discrete approximation is

then formed using one or another finite-difference scheme. In contrast to this method, [11–18] used an approach called discrete, in which the governing equations are initially discretized and then linearized.

The Jacobian matrices obtained using these approaches differ, since in general the linearization and discretization operations are noncommutative [10]. However, as the mesh is refined, the difference between the results of these approaches should decrease. Different aspects of the continuum and discrete approaches have been studied in the context of solving conjugate equations for optimization problems [19, 20]. However, these approaches were not compared within the framework of GSA in the literature and the choice of a specific approach in [5– 18] was not substantiated.

The goal of this study consists in comparing the results of GSA using various methods for calculating the Jacobian matrix using the example of laminar flow around a cylinder with perfect gas at near-critical Reynolds numbers.

Global stability analysis of steady laminar flows

The procedure for studying the global stability of laminar flows contains two main stages.

The first one is finding a numerical solution of a generalized system of steady Navier–Stokes equations, including equations of continuity, conservation of motion and energy, which can be written in operator form:

$$R(q) = 0, \tag{1}$$

where $q = \{\rho, \rho u, \rho v, \rho E\}^T$ is the vector of conservative variables; R is the nonlinear differential operator of steady Navier–Stokes equations.

The solution of the steady Navier–Stokes equations satisfying Eq. (1) and obtained by analyzing the stability of the flow is often called the basic one. The stability of this solution, denoted as $\underline{q}$, is in fact the subject of our analysis.

At the second stage, the evolution of perturbations of the basic solution over time is considered. The equation for perturbations can be obtained from the transient Navier–Stokes equations; they are written in the following operator form:

$$\frac{\partial q}{\partial t} = -R(q). \tag{2}$$

GSA uses the traditional approach for linear stability analysis, which is based on representation of the solution of the system of equations (2) as the sum of its steady solution $\bar{q}$ and small perturbations q':

$$q = \bar{q} + q'. \tag{3}$$

To obtain equations that are linear with respect to q', linearization of the operator $R(q)$ is carried out in the vicinity of the basic solution for these perturbations:

$$R(\bar{q} + q') = R(\bar{q}) + \frac{\partial R}{\partial q}(\bar{q})q', \tag{4}$$

where $\frac{\partial R}{\partial q}(\bar{q}) \equiv J(\bar{q})$ is the Jacobian of the Navier–Stokes equations (a differential operator depending on the basic solution).

The equation of relatively small perturbations is obtained by substituting expansion (3) into Eq. (2), taking into account Eqs. (1) and (4):

$$\frac{\partial q'}{\partial t} + J(\bar{q})q' = 0. \tag{5}$$

Due to linearity of the system of differential equations (5), its general solution is represented as a sum of terms (modes of perturbations), each of which is also a solution of system (5). Each mode can be represented as

$$q'(x,y,t) = \hat{q}(x,y)\exp(\omega t), \tag{6}$$

where $\hat{q}$ is the complex vector of the perturbation amplitudes; ω is the complex number $\omega_r + i\omega_i$, whose real part ω_r is the rate of growth/attenuation of the perturbation, and the imaginary part ω_i is its frequency (only the real part of relation (6) has a physical meaning).

Substituting equality (6) into system (5) leads to the eigenvalue problem for the Jacobian of the governing equations:

$$J\hat{q} = \omega\hat{q}. \tag{7}$$

The numerical solution of this problem is carried out on a finite difference mesh, so all continuous vectors and operators are replaced by their discrete approximations. Discretization of derivatives at each point of the computational mesh in accordance with an existing stencil of a numerical scheme determines the dependence of these derivatives on the values of variables at adjacent points. Thus, problem (7) is reduced to the eigenvalue problem of the discrete approximation of the Jacobian J, that is, the matrix M_{kl}:

$$M_{kl}\hat{\alpha}_l = \omega\hat{\alpha}_k. \tag{8}$$

Here, the vector $\hat{\alpha}_l$ is the discretized field of the amplitude of perturbations $\hat{q}$, and the discretized Jacobian M_{kl} is the matrix of derivative equations with respect to all variables at all points of the computational mesh, therefore, the indices k and l in Eq. (8) take values from 1 to $N_p \times N_v$, where N_p is the number of nodes of the computational mesh, N_v is the number of variables.

It should be noted that instead of linearization of expression (7) at the boundary points of the computational domain, linearization of the corresponding boundary conditions is used, therefore, the following equation is used for these points, instead of expression (8):

$$M_{kl}\hat{\alpha}_l = 0. \tag{9}$$

Eqs. (8), (9) can be combined if we formulate a generalized eigenvalue problem:

$$M_{kl}\hat{\alpha}_l = \omega T_{km}\hat{\alpha}_m, \tag{10}$$

where T_{km} is a diagonal matrix with $T_{ii} = 0$ at the boundary points and $T_{ii} = 1$ at the inner points.

Thus, the determination of the stability of the flow within the framework of GSA is reduced to solving the generalized eigenvalue problem (10). The eigenvalues of the matrix M_{kl} correspond to different modes of perturbation, and the real part of the eigenvalues is equal to the rate of growth of perturbations, and the imaginary part is the frequency of their vibrations.

The eigenvectors correspond to the spatial distributions of the mode amplitudes. The flow is unsteady if at least one eigenvalue has a positive real part (i.e., there is a growing perturbation mode), and stable otherwise.

As already noted in the introduction, two different approaches are currently used to determine the elements of the M_{kl} matrix at the inner points of the computational domain. According to the method for calculating this matrix, the GSA is called continuum or discrete, respectively.

Within the framework of the first of approach (see, for example, [5]), called continuum in [10], an analytical expression is derived for the Jacobian J, and then its discretization is carried out using some numerical scheme, which, generally speaking, may differ from that used to solve system of equations (1) obtaining the basic solution.

In contrast, within the second approach (see, for example, [11, 12]), called discrete in [10], the calculation of the Jacobian in problem (7) is carried out not at the differential, but at the discrete level, i.e., it is not the operator R itself that is differentiated, but its discrete form, used to obtain

a basic solution, called the right-hand side of system (2) (traditionally denoted as RHS_k); index k takes values from 1 to $N_p \times N_v$, as in Eq. (10).

The discrete form of the Jacobian in this case is the matrix of partial derivatives RHS_k with respect to the variables α_l (the discrete form of the vector of the principal variables q) at each inner point of the computational mesh:

$$M_{kl} = \frac{\partial \mathrm{RHS}_k}{\partial \alpha_l}. \tag{11}$$

There are two approaches to differentiating Eq. (11). Within the framework of the first, the explicit dependence $\mathrm{RHS}_k(\alpha_l)$ is formulated for the numerical scheme used, and then differentiated analytically. Even though this problem is very time-consuming, especially for modern schemes with high-order accuracy, it was solved in [21], and the developed approach was successfully applied in [11, 13, 16, 18].

This paper uses an alternative approach based on the technology of automatic differentiation (AD). Even though AD as a concept has appeared quite long ago [22], interest in it arose only in the last two decades, with efforts to solve related problems on optimizing the shapes of airfoils [23].

The basis for the AD is that the algorithm for calculating any complex function (including RHS) consists of sequential application of elementary operations φ_1 (addition, multiplication, exponentiation, etc.):

$$\mathrm{RHS} = \varphi_1 \circ \varphi_2 \circ \ldots \circ \varphi_n. \tag{12}$$

The values of the derivative of the elementary function at each step are known analytically, so the Jacobian of the RHS function can be calculated by the rule of differentiation of a complex function:

$$J = \varphi_1' \circ \varphi_2' \circ \ldots \circ \varphi_n'. \tag{13}$$

Libraries implementing AD (see, for example, [24, 25]) accumulate the results of this differentiation during the calculation of the initial function and calculate the discretized Jacobian. Notably, the AD method is not automatic in the full sense of the word and requires editing the source code of the program.

In the absence of gas-dynamic discontinuities, theoretically (i.e., with computational meshes that provide grid-independent solutions for emerging perturbations), the continuum and discrete approaches should provide the same result. However, in practice, the results obtained using different approaches on finite grids may differ dramatically.

It should be noted that the evolution of perturbations can be considered not only within the GSA, but also within direct numerical simulation of transient Navier–Stokes equations (2). In this case, the solution of the steady Navier–Stokes equations (1) is used as an initial approximation. The initial perturbations are determined by the error of the numerical solution of transient equations. If the flow is unsteady, then an increase in the amplitude of perturbations is observed as a result of the calculation. At the linear stage, when the exponential nature of the growth of perturbations is observed, their evolution should be consistent with the results of the GSA in the discrete calculation of the Jacobian.

In this paper, we verified our implementation of the discrete approach to calculating the Jacobian based on such a comparison.

Statement of the problem on the stability of steady flow around a cylinder and its computational aspects

The results of two stability analysis methods were compared using the example of the problem on laminar flow around a cylinder with perfect gas, using meshes that are sequentially refined in both directions. The problem was considered in a compressible statement with the Mach number M = 0.2 and two values of the Reynolds number, Re = 50 and 60, slightly exceeding the Reynolds

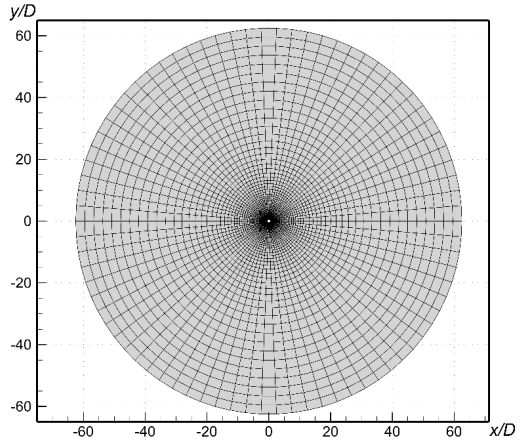

Fig. 1. Example of *O*-type computational mesh (*L*1 mesh)

number for the stability threshold, Re ≈ 47 (see, for example, [26]), when the Reynolds number is constructed from the velocity of the incident flow U_0 and the diameter of the cylinder *D*.

The size of the computational domain was 120*D*. This size was sufficient to eliminate the influence of boundary conditions on the basic solution and the results of the GSA. A series of *O*-type computational meshes was constructed in this region (an example of such a mesh is shown in Fig. 1) with a uniform distribution of nodes along the angular coordinate and clustering towards the wall along the radial coordinate (the parameters of the constructed meshes are shown in Table 1).

In this paper, the finite volume Numerical Turbulence Simulation (NTS) CFD code was used for calculations [27]. In this code, the finite-difference relaxation method is used to find steady solutions to the governing equations. A hybrid scheme is used to approximate inviscid flows in calculations of compressible flows:

$$\Delta_H = \alpha_U \Delta_{Roe} + (1 - \alpha_U)\Delta_{4C}, \tag{14}$$

where α_U is the weight of upwind approximation; Δ_{Roe}, Δ_{4C} are the finite difference operators of the third-order upwind-biased Roe scheme and the fourth-order central difference scheme, respectively.

Table 1

Parameters of O-type computational meshes used and their values

Mesh	N_φ	N_r	$\Delta h_1/D$	$\Delta h_{i+1}/\Delta h_i$	$\Delta h_{\max}/D$
*L*1	80		$1.0\cdot10^{-2}$	1.098	2
*L*2	160		$5.0\cdot10^{-3}$	1.040	2
*L*3	240		$2.5\cdot10^{-3}$	1.028	2
*L*4	320		$1.0\cdot10^{-3}$	1.023	2
*L*5	800		$1.0\cdot10^{-4}$	1.011	1

Notations: N_φ, N_r is the number of nodes in the circumferential and radial directions, respectively, Δh_i is the grid pitch, $\Delta h_{\max}$ is its maximum value, *D* is the diameter of the cylinder.

The viscous components of the flows are approximated using a second-order central difference scheme.

To calculate the evolution of small perturbations by solving transient Navier–Stokes equations, numerical time integration was carried out using an implicit second-order Euler scheme with a time step $\Delta t = 0.3\cdot D/U_0$, which provided values of the Courant number less than unity in almost the entire computational domain and approximately 1,000 steps per Kármán vortex street for all meshes.

The indicators of the growth or attenuation of perturbations and their frequency were determined by processing the dependences of the transverse velocity on time obtained by unsteady calculations at several points in space. A linear stage of perturbation evolution was identified, when their amplitude increases exponentially.

Solving the spectral problem, the calculation of the discrete form of the Jacobian was carried out by both methods (discrete and continuum). Within the framework of the continuum method

implemented earlier in the NTS code, a finite-difference scheme was used to discretize the Jacobian J (it is described in more detail in [5]), which is a combinations of a third-order upwind scheme and a fourth-order central difference scheme:

$$\Delta_H = \alpha_U \Delta_{3U} + (1 - \alpha_U)\Delta_{4C}, \tag{15}$$

where α_U is the weight of the upwind approximation; Δ_{3U}, Δ_{4C} are the finite difference operators of the upwind scheme and the central difference scheme, respectively.

To use the discrete approach, we implemented in this paper, we applied the automatic differentiation method (using the ADF95 library [25]). For the numerical solution of the eigenvalue problem, the Krylov–Schur method was used, which is implemented using the open library SPEPc/PETSc [28]. This method is designed to solve eigenvalue problems with sparse non-Hermitian matrices of large size (this is the type of matrix considered). It is a modification of an implicitly restarted version of the Arnoldi method, which belongs to the class of Rayleigh–Ritz methods based on projection onto the Krylov subspace (see, for example, monograph [29]). The Krylov–Schur method allows to obtain the requested number of the eigenvalues the largest in absolute value and their corresponding eigenvectors. Therefore, to use it, the initial matrix is pre-transformed in such a way that the most important eigenvalues in terms of stability with the largest real part become the largest in absolute value. This transformation is a combination of shifting and inverting the matrix (this approach is called the "Shift-Invert Approach" in the literature [30]).

Verification of the GSA results obtained with the discrete approach to calculating the Jacobian

Fig. 2 shows the spatial distributions of perturbations of the longitudinal velocity U' at the Reynolds number Re = 60 on the *L4* mesh, obtained by discrete GSA and direct numerical solution of the transient Navier–Stokes equations. For the latter, the local amplitudes of perturbations are obtained as a result of subtracting the fields of the instantaneous and basic solution with normalization to the maximum value $|U'_{\max}|$.

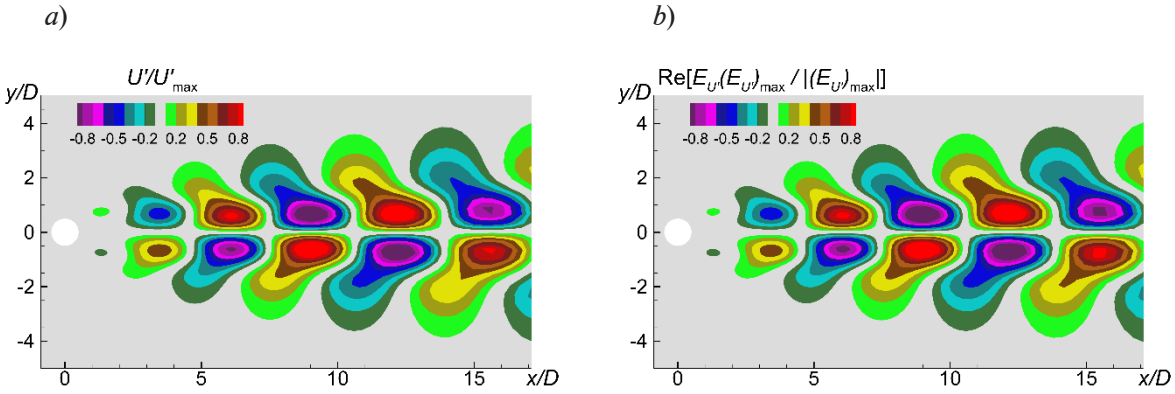

Fig. 2. Spatial distributions of longitudinal velocity perturbations obtained on the *L4* mesh by direct numerical solution of the transient Navier–Stokes equations (*a*) and using discrete GSA (*b*)
Reynolds number Re = 60, Mach number M = 0.2

In the framework of a discrete GSA, the spatial distribution of perturbations is determined by the real component of the eigenvector corresponding to the most unstable eigenvalue. For comparison, the complex components of the E_U vectors corresponding to the longitudinal velocity perturbations were reduced in phase and amplitude to the value at the point where the amplitude of the perturbations $|U'_{\max}|$ is maximum. The analysis of the data in Fig. 2 allows us to conclude the discrete GSA not only correctly predicts the shape of perturbations developing due to instability on the *L4* mesh but also provides good quantitative agreement.The growth rate and the frequency of development of the most unstable perturbations at Re = 60 on a series of meshes

$L1-L5$ are shown in Table 2. The growth rate and frequency obtained by the discrete approach coincide with high accuracy (on all meshes for the flow, the error does not exceed 0.4%) with the solution of the transient Navier–Stokes equations, which indicates that the approach was implemented correctly.

Table 2

Comparison of computational parameters of the most unstable perturbations obtained by two methods on a series of meshes

Mesh	Computational value of parameter			
	Growth rate ω_r		Frequency ω_i	
	I	II	I	II
$L1$	0.0132		0.754	0.753
$L2$	0.0389		0.740	0.741
$L3$	0.0420	0.0421	0.738	
$L4$	0.0430	0.0431	0.737	
$L5$	0.0437		0.736	

Notations: I corresponds to direct numerical solution of transient Navier–Stokes equations; II to GSA, discrete approach. Note. Reynolds number Re = 60, Mach number M = 0.2.

Comparison of the results of two methods of global stability analysis

The direct comparison of the discrete and continuum approaches implemented in the NTS code is complicated by differences both in the methods for calculating the Jacobian and in the numerical schemes used to calculate the inviscid part of the flows.

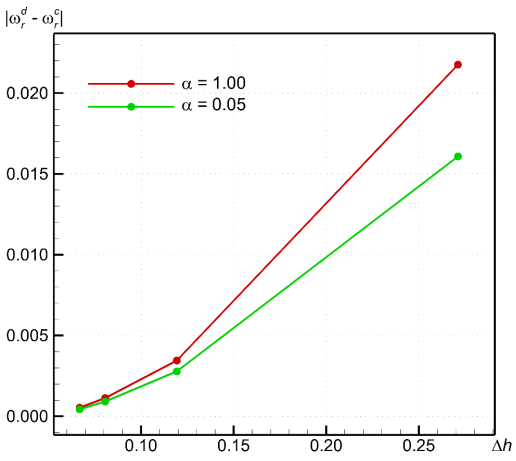

Fig. 3. Effect of the grid step on the difference in growth rates ω_r calculated using discrete (d) and continuum (c) GSA methods
Hybrid schemes with two weights of the upwind term α were used

The discrete GSA uses the same computational scheme as for calculating the basic flow, i.e., a hybrid upwind Roe scheme. This correction is significantly nonlinear, which does not allow it to be used within the framework of continuum GSA, therefore it uses a simplified linear upwind term. It would be possible to avoid differences between the schemes by using identical central difference schemes, but in practice this is impossible due to loss of stability when obtaining a basic solution. Nevertheless, if we reduce the weight of the upwind term, this can drastically reduce the difference in the schemes used.

This possibility is illustrated in Fig. 3, which shows the dependence on the grid step of the modulo difference in growth indicators $|\omega_r^d - \omega_r^c|$ in the vicinity of the cylinder obtained from the results of discrete and continuum GSA. If the weight of the upwind term is reduced, the difference decreases. The following are the results obtained using hybrid schemes with the weight of the upwind term $\alpha = 0.05$.

The growth rate and frequency obtained on the smallest $L5$ grid using the continuum and discrete approaches (Table 3) practically coincide. The same table shows a comparison with the results from [26, 31], confirming that the GSA results are representative.

Table 3

Comptutational parameters of unsteady perturbation mode obtained by two methods on the *L*5 mesh with varying Reynolds numbers, as well as comparison with the literature data

Computational approach	Computational value of parameter			
	ω_r		ω_i	
	Re=50	Re=60	Re=50	Re=60
GSA, discrete approach	–0.01099	–0.04368	0.72965	0.73637
continuum	–0.01093	–0.04372	0.72955	0.73633
[26], GSA, discrete approach	–0.013	–0.047	0.745	0.754
[31], direct numerical solution of Navier–Stokes equations	–0.012	–0.050	0.750	0.757

The arithmetic mean of the eigenvalues obtained using discrete and continuum approaches was used as a "reference" value of $\omega^{ref} = \left(\omega_r^{ref}, \omega_i^{ref}\right)$ to estimate the error in calculating the growth rate and the frequency of unsteady perturbation mode on on the coarser mesh *L*5.

Dependences of the error of the GSA results

$$\Delta\omega = \frac{(\omega - \omega^{ref})D}{U_0}$$

on the characteristic step of the mesh Δh, defined as the average step along the angular coordinate at a distance of 4*D* from the surface of the cylinder, are shown in Fig. 4 and allow us to draw the following conclusions.The calculation error is almost the same for both considered Reynolds numbers. The real order of accuracy of the GSA, which was determined by power-law approximations of the dependence of the error on the grid step, turned out to be approximately the same for both approaches: its value is approximately 3.1 for the growth rate, and 1.8 (discrete GSA) and 2.0 (continuum GSA) for frequency. These values are consistent with the formal order of the

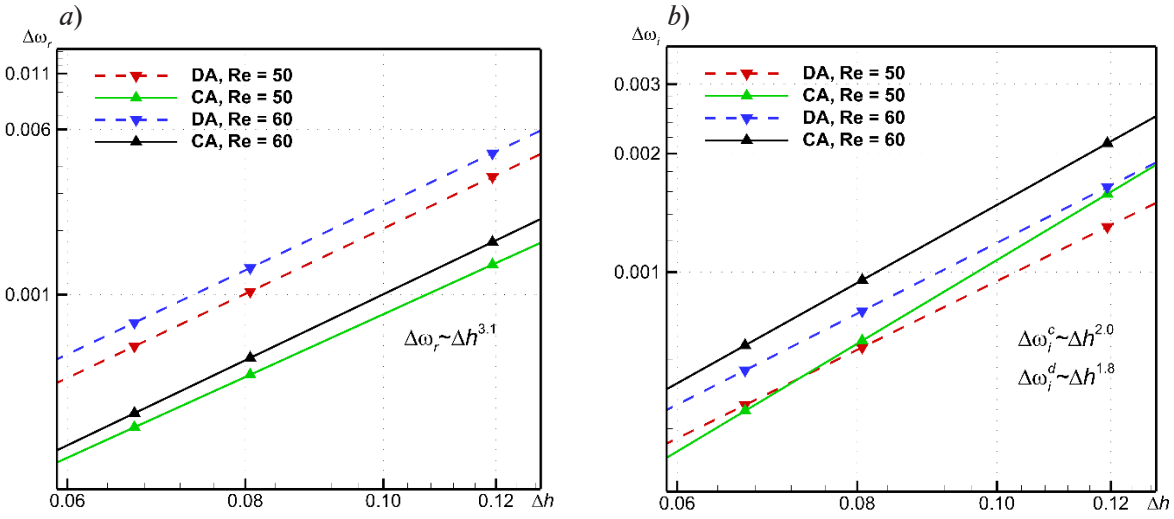

Fig. 4. Stepwise dependences of errors in calculating the growth rate (*a*) and frequency (*b*). The dependences were obtained by discrete (DA) and continuum (CA) approaches on meshes *L*1 – *L*4, with varying Reynolds numbers (dependences are given by symbols), and their approximation by exponential functions (straight lines on a logarithmic scale)

schemes used, in which convective terms are approximated by the third order, and viscous ones by the second. In addition, it should be borne in mind that the actual order of the schemes may decrease on non-uniform meshes (that is, the meshes are used in this work). The analysis of the data in Fig. 4 also allows us to conclude that the error in predicting the growth rate was about three times less when using the continuum approach, and the error in predicting the frequency of perturbations was less when using the discrete approach.

Conclusion

Two approaches to global stability analysis (GSA) were compared using the example of the problem on laminar flow around a cylinder at Reynolds numbers close to critical, differing in the methods for calculating the Jacobian of the Navier–Stokes equations: discrete (linearization of these discretized equations) and continuum (discretization of these linearized equations).

The discrete GSA approach we implemented was verified by comparison with the results of direct numerical simulation of unsteady laminar flow around the cylinder at Reynolds number $\mathrm{Re} = 60$. The results of the comparison showed that the growth rate and the vibration frequency of the most unsteady mode coincided with high accuracy on all the considered meshes.

The order of accuracy of the GSA turned out to be the same for continuum and discrete methods for calculating the Jacobian, and corresponded to the formal order of accuracy of spatial discretization by the numerical schemes used to obtain the solution whose stability was analyzed The error in predicting the growth rate of perturbations is less when using the continuum approach, and the error in predicting the vibration frequency of perturbations is less when using the discrete approach.

Thus, it can be argued that the continuum and discrete approaches are equivalent in order of accuracy and the choice of a specific approach for conducting stability analysis can be determined by other criteria (ease of implementation, computational costs, etc.).

This study was supported by the Russian Science Foundation (grant 21-72-20029). The simulations were run on the Polytechnic RSC Tornado cluster of the Polytechnic Supercomputer Center (http://www.scc.spbstu.ru).

REFERENCES

1. **Boiko A. V., Dovgal A. V., Grek G. R., Kozlov V. V.,** Physics of transitional shear flows: Instability and laminar-turbulent transition in incompressible near-wall shear layers, Book Ser. “Fluid Mechanics and its Applications”, Springer, 2012.

2. **Schmid P. J., Henningson D. S.,** Stability and transition in shear flows, Book Series “Applied Mathematical Sciences”, Vol. 142. Springer, New York, 2001.

3. **Theofilis V.,** Advances in global linear instability analysis of nonparallel and three-dimensional flows, Prog. Aerosp. Sci. 39 (4) (2003) 249–315.

4. **Theofilis V.,** Global linear instability, Annu. Rev. Fluid Mech. 43 (2011) 319–352.

5. **Crouch J. D., Garbaruk A., Magidov D.,** Predicting the onset of flow unsteadiness based on global instability, J. Comput. Phys. 224 (2) (2007) 924–940.

6. **Crouch J. D., Garbaruk A., Magidov D., Travin A.,** Origin of transonic buffet on aerofoils, J. Fluid Mech. 628 (10 June) (2009) 357–369.

7. **Garbaruk A., Crouch J. D.,** Quasi-three-dimensional analysis of global instabilities: Onset of vortex shedding behind a wavy cylinder, J. Fluid Mech. 677 (25 June) (2011) 572–588.

8. **Crouch J. D., Garbaruk A., Strelets M.,** Global instability in the onset of transonic-wing buffet, J. Fluid Mech. 881 (25 Dec.) (2019) 3–22.

9. **Garbaruk A., Strelets M., Crouch J. D.,** Effects of extended laminar flow on wing buffet-onset characteristics, AIAA J. 59 (8) (2021) 2848–2854.

10. **De Pando M. F., Sipp D., Schmid P. J.,** Efficient evaluation of the direct and adjoint linearized dynamics from compressible flow solvers, J. Comput. Phys. 231 (23) (2012) 7739–7755.

11. **Thormann R., Widhalm M.,** Linear-frequency-domain predictions of dynamic-response data for viscous transonic flows, AIAA J. 51 (11) (2013) 2540–2557.

12. **Mettot C., Renac F., Sipp D.,** Computation of eigenvalue sensitivity to base flow modifications in a discrete framework: Application to open-loop control, J. Comput. Phys. 269 (15 July) (2014) 234–258.

13. **Xu S., Timme S., Badcock K. J.,** Krylov subspace recycling for linearized aerodynamics analysis using DLR-TAU, Proc. Int. Forum Aeroelasticity Struct. Dyn. (IFASD 2015). 28 June–2 July, 2015. St. Petersburg, Russia. In 3 Vols. 2 (2016) 1462–1479.

14. **Sartor F., Metot C., Bur R., Sipp D.,** Unsteadiness in transonic shock-wave/boundary-layer interactions: experimental investigation n and global stability analysis, J. Fluid Mech. 781 (25 Oct.) (2015) 550–577.

15. **Busquet D., Marquet O., Richez F., et al.,** Global stability analysis of turbulent flows around an airfoil near stall, Proc. Eurogen 2017 Conf., Sept. 13–15, 2017, Madrid, Spain. Pp. 1–7.

16. **Timme S.,** Global instability of wing shock-buffet onset, J. Fluid Mech. 885 (25 Febr.) (2020) P. A37.

17. **Plante F., Dandois J., Beneddine S., et al.,** Link between subsonic stall and transonic buffet on swept and unswept wings: From global stability analysis to nonlinear dynamics, J. Fluid Mech. 908 (10 Febr.) (2021) A16.

18. **He W., Timme S.,** Triglobal infinite-wing shock-buffet study, J. Fluid Mech. 925 (25 Oct.) (2021) A27.

19. **Giles M. B., Pierce N. A.,** An introduction to the adjoint approach to design, Flow, Turbul. Combust. 65 (3–4) (2000) 393–415.

20. **Peter J. E. V., Dwight R. P.,** Numerical sensitivity analysis for aerodynamic optimization: A survey of approaches, Comput. Fluids. 39 (3) (2010) 373–391.

21. **Dwight R. P.,** Efficiency improvements of RANS-based analysis and optimization using implicit and adjoint methods on unstructured grids, Dtsch. Zent. fur Luft-und Raumfahrt–Forschungsberichte. (11) (2006) 1–162.

22. **Wengert R. E.,** A simple automatic derivative evaluation program, Commun. ACM. 7 (8) (1964) 463–464.

23. **Lyu Z., Kenway G. K. W.,** Automatic differentiation adjoint of the Reynolds-averaged Navier–Stokes equations with a turbulence model, Proc. 21st AIAA Comput. Fluid Dyn. Conf., June 24–27, 2013. San Diego (USA) (2013) 1–24.

24. **Hascолт L., Pascual V.,** TAPENADE 2.1 user's guide, INRIA Tech. Rep. No. 0300. Sept. 2004. 78 p. http://www.inria.fr/rrrt/rt-0300.html.

25. **Straka C. W.** ADF95: Tool for automatic differentiation of a FORTRAN code designed for large numbers of independent variables, Comput. Phys. Commun. 168 (2) (2005) 123–139.

26. **Gianetti F., Luchini P.,** Structural sensitivity of the first instability of the cylinder wake, J. Fluid Mech. 581 (25 June) (2007) 167–197.

27. **Shur M. L., Strelets M. K., Travin A. K.,** High-order implicit multi-block Navier – Stokes code: Ten-year experience of application to RANS / DES / LES / DNS of turbulence, Proc. 7th Symp. Overset Grids Solut. Technol. Oct. 5–7, 2004. Huntington Beach, CA, USA (2004) 1–52.

28. **Hernandez V., Roman J. E., Vidal V.,** SLEPC: A scalable and flexible toolkit for the solution of eigenvalue problems, ACM Trans. Math. Softw. 31 (3) (2005) 351–362.

29. **Golub G. H., van Loan C. F.,** Matrix computations, 3-rd Ed., John Hopkins University Press, Baltimore, Maryland, USA,1996.

30. **Mack C. J., Schmid P. J.,** A preconditioned Krylov technique for global hydrodynamic stability analysis of large-scale compressible flows, J. Comput. Phys. 229 (3) (2010) 541–560.

31. **Canuto D., Taira K.,** Two-dimensional compressible viscous flow around a circular cylinder, J. Fluid Mech. 785 (25 Dec.) (2015) 349–371.

СПИСОК ЛИТЕРАТУРЫ

1. **Бойко А. В., Грек Г. Р., Довгаль А. В., Козлов В. В.** Физические механизмы перехода к турбулентности в открытых течениях. Москва-Ижевск: НИЦ «Регулярная и хаотическая динамика», Институт компьютерных исследований, 2006. 304 с.

2. **Schmid P. J., Henningson D. S.** Stability and transition in shear flows. Book Series "Applied mathematical Sciences", Vol. 142. New York: Springer, 2001. 556 p.

3. **Theofilis V.** Advances in global linear instability analysis of nonparallel and three-dimensional flows // Progress in Aerospace Sciences. 2003. Vol. 39. No. 4. Pp. 249–315.

4. **Theofilis V.** Global linear instability // Annual Review of Fluid Mechanics. 2011. Vol. 43. Pp. 319–352.

5. **Crouch J. D., Garbaruk A., Magidov D.** Predicting the onset of flow unsteadiness based on global instability // Journal of Computational Physics. 2007. Vol. 224. No. 2. Pp. 924–940.

6. **Crouch J. D., Garbaruk A., Magidov D., Travin A.** Origin of transonic buffet on aerofoils // Journal of Fluid Mechanics. 2009. Vol. 628. 10 June. Pp. 357–369.

7. **Garbaruk A., Crouch J. D.** Quasi-three-dimensional analysis of global instabilities: Onset of vortex shedding behind a wavy cylinder // Journal of Fluid Mechanics. 2011. Vol. 677. 25 June. Pp. 572–588.

8. **Crouch J. D., Garbaruk A., Strelets M.** Global instability in the onset of transonic-wing buffet // Journal of Fluid Mechanics. 2019. Vol. 881. 25 December. Pp. 3–22.

9. **Garbaruk A., Strelets M., Crouch J. D.** Effects of extended laminar flow on wing buffet-onset characteristics // AIAA Journal. 2021. Vol. 59. No. 8. Pp. 2848–2854.

10. **De Pando M. F., Sipp D., Schmid P. J.** Efficient evaluation of the direct and adjoint linearized dynamics from compressible flow solvers // Journal of Computational Physics. 2012. Vol. 231. No. 23. Pp. 7739–7755.

11. **Thormann R., Widhalm M.** Linear-frequency-domain predictions of dynamic-response data for viscous transonic flows // AIAA Journal. 2013. Vol. 51. No. 11. Pp. 2540–2557.

12. **Mettot C., Renac F., Sipp D.** Computation of eigenvalue sensitivity to base flow modifications in a discrete framework: Application to open-loop control // Journal of Computational Physics. 2014. Vol. 269. 15 July. Pp. 234–258.

13. **Xu S., Timme S., Badcock K. J.** Krylov subspace recycling for linearized aerodynamics analysis using DLR-TAU // Proceedings of the International Forum on Aeroelasticity and Structural Dynamics (IFASD 2015). 28 June–2 July, 2015. St. Petersburg, Russia. In 3 volumes. Vol. 2. Pp. 1462–1479.

14. **Sartor F., Metot C., Bur R., Sipp D.** Unsteadiness in transonic shock-wave/boundary-layer interactions: experimental investigation n and global stability analysis // Journal of Fluid Mechanics. 2015. Vol. 781. 25 October. Pp. 550–577.

15. **Busquet D., Marquet O., Richez F., Juniper M., Sipp D.** Global stability analysis of turbulent flows around an airfoil near stall // Proceedings of the Eurogen 2017 Conference. September 13–15, 2017. Madrid, Spain. Pp. 1–7.

16. **Timme S.** Global instability of wing shock-buffet onset // Journal of Fluid Mechanics. 2020. Vol. 885. 25 February. P. A37.

17. **Plante F., Dandois J., Beneddine S., Laurendeau E., Sipp D.** Link between subsonic stall and transonic buffet on swept and unswept wings: From global stability analysis to nonlinear dynamics // Journal of Fluid Mechanics. 2021. Vol. 908. 10 February. P. A16.

18. **He W., Timme S.** Triglobal infinite-wing shock-buffet study // Journal of Fluid Mechanics. 2021. Vol. 925. 25 October. P. A27.

19. **Giles M. B., Pierce N. A.** An introduction to the adjoint approach to design // Flow, Turbulence and Combustion. 2000. Vol. 65. No. 3–4. Pp. 393–415.

20. **Peter J. E. V., Dwight R. P.** Numerical sensitivity analysis for aerodynamic optimization: A survey of approaches // Computers & Fluids. 2010. Vol. 39. No. 3. Pp. 373–391.

21. **Dwight R. P.** Efficiency improvements of RANS-based analysis and optimization using implicit and adjoint methods on unstructured grids // Deutsches Zentrum fьr Luft-und Raumfahrt – Forschungsberichte. 2006. No. 11. Pp. 1–162.

22. **Wengert R. E.** A simple automatic derivative evaluation program // Communications of the ACM. 1964. Vol. 7. No. 8. Pp. 463–464.

23. **Lyu Z., Kenway G. K. W.** Automatic differentiation adjoint of the Reynolds-averaged Navier–Stokes equations with a turbulence model // Proceedings of the 21st AIAA Computational Fluid Dynamics Conference. June 24–27, 2013. San Diego (USA), Pp. 1–24.

24. **Hascoлt L., Pascual V.** TAPENADE 2.1 user's guide. INRIA Technical Report No. 0300. September, 2004. 78 p. http://www.inria.fr/rrrt/rt-0300.html

25. **Straka C. W.** ADF95: Tool for automatic differentiation of a FORTRAN code designed for large numbers of independent variables // Computer Physics Communications. 2005. Vol. 168. No. 2. Pp. 123–139.

26. **Gianetti F., Luchini P.** Structural sensitivity of the first instability of the cylinder wake // Journal of Fluid Mechanics. 2007. Vol. 581. 25 June. Pp. 167–197.

27. **Shur M. L., Strelets M. K., Travin A. K.** High-order implicit multi-block Navier – Stokes code: Ten-year experience of application to RANS / DES / LES / DNS of turbulence // Proceedings of

the 7th Symposium on Overset Grids & Solution Technology. October 5–7, 2004. Huntington Beach, CA, USA. 2004. Pp. 1–52.

28. **Hernandez V., Roman J. E., Vidal V.** SLEPC: A scalable and flexible toolkit for the solution of eigenvalue problems // ACM Transactions of Mathematical Software. 2005. Vol. 31. No. 3. Pp. 351–362.

29. **Голуб Дж., Лоун Ван Ч.** Матричные вычисления. Пер. с англ. Под ред. Воеводина В. В. М.: Мир, 1999. 548 с.

30. **Mack C. J., Schmid P. J.** A preconditioned Krylov technique for global hydrodynamic stability analysis of large-scale compressible flows // Journal of Computational Physics. 2010. Vol. 229. No. 3. Pp. 541–560.

31. **Canuto D., Taira K.** Two-dimensional compressible viscous flow around a circular cylinder // Journal of Fluid Mechanics. 2015. Vol. 785. 25 December. Pp. 349–371.

THE AUTHORS

GOLUBKOV Valentin D.
Peter the Great St. Petersburg Polytechnic University
29 Politechnicheskaya St., St. Petersburg, 195251, Russia
golubkovvd@gmail.com
ORCID: 0000-0001-9473-7430

GARBARUK Andrey V.
Peter the Great St. Petersburg Polytechnic University
29 Politechnicheskaya St., St. Petersburg, 195251, Russia
agarbaruk@mail.ru
ORCID: 0000-0002-2775-9864

СВЕДЕНИЯ ОБ АВТОРАХ

ГОЛУБКОВ Валентин Денисович – *инженер лаборатории «Вычислительная гидроакустика и турбулентность» Высшей школы прикладной математики и вычислительной физики Санкт-Петербургского политехнического университета Петра Великого.*
195251, Россия, г. Санкт-Петербург, Политехническая ул., 29
golubkovvd@gmail.com
ORCID: 0000-0001-9473-7430

ГАРБАРУК Андрей Викторович – *доктор физико-математических наук, главный научный сотрудник лаборатории «Вычислительная гидроакустика и турбулентность» Высшей школы прикладной математики и вычислительной физики Санкт-Петербургского политехнического университета Петра Великого.*
195251, Россия, г. Санкт-Петербург, Политехническая ул., 29
agarbaruk@mail.ru
ORCID: 0000-0002-2775-9864

Received 20.12.2022. Approved after reviewing 26.09.2023. Accepted 26.09.2023.
Статья поступила в редакцию 20.12.2022. Одобрена после рецензирования 26.09.2023. Принята 26.09.2023.